Available online at www.sciencedirect.com
ScienceDirect
Journal of Molecular Catalysis A: Chemical 267 (2007) 245–254
JOURNAL OF MOLECULAR CATALYSIS A: CHEMICAL
www.elsevier.com/locate/molcata

The study on the source of Te and the dispersion of TeO_2 in fabricating Mo–V–Te and Mo–V–Te–Nb mixed metal oxide catalysts for propane partial oxidation

Ru-Ming Feng [a], Xiu-Juan Yang [a], Wei-Jie Ji [a,*], Hai-Yang Zhu [a], Xiao-Dong Gu [a], Yi Chen [a], Scott Han [b], Hartmut Hibst [c]

[a] *Key Laboratory of Mesoscopic Chemistry, MOE, School of Chemistry and Chemical Engineering, Nanjing University, Nanjing 210093, China*
[b] *Rohm & Haas Company, Philadelphia, PA 19106-2399, USA*
[c] *BASF Aktiengesellschaft, 67056 Ludwigshafen, Germany*

Received 24 October 2006; received in revised form 25 November 2006; accepted 28 November 2006
Available online 3 December 2006

Abstract

The effects of the source of Te and the dispersion of TeO_2 on fabricating Mo–V–Te and Mo–V–Te–Nb mixed metal oxide (MMO) catalysts for propane partial oxidation to acrylic acid (AA) were systematically studied. In order to modify the dispersion of TeO_2 in the preparation medium, wet-milling and ultrasonic-assisted dispersion of TeO_2 were adopted. The selected samples were characterized by means of BET, XRD, ICP/XRF, XPS, SEM, H_2- and C_3H_8-TPR and calorimetric NH_3 adsorption. It was clearly demonstrated that different sources of Te and dispersion of TeO_2 in preparation showed significant impact on the physicochemical properties (phase composition, bulk/surface elemental concentration, reactivity of lattice oxygen, and surface acidity) and catalytic activity of the MMO catalysts. The employment of ultrasonic treatment was proved to be effective for making more active and selective Mo–V–Te/Mo–V–Te–Nb catalysts for the target action.

Keywords: Catalyst fabrication; Te source; Dispersion of TeO_2; Mixed metal oxides; Propane oxidation

1. Introduction

Adopting cheap, abundant and environmentally friendly feed stock such as paraffins instead of traditionally used olefins and aromatic hydrocarbons is desirable [1–3]. The challenge in alkane oxidation, however, is how to increase the selectivity of target products [4]. To make full use of light alkanes (C_1–C_4) in natural gas to produce essential chemicals is one of the most important strategies for future chemical society.

Acrylic acid (AA) is an essential chemical and widely used for production of esters, polyesters, amides, anilides, etc. The current process for AA production involves two separate steps [5]. However, one-step partial oxidation of propane to AA is highly desirable and has derived numerous attentions in recent years [6–51]. There are three types of catalysts have been investigated so far for the reaction, namely, vanadium phosphorus oxides [6–9], heteropoly compounds [10–13] and mixed metal oxides [16–51]. Although higher AA yield (>40%) can be obtained over the mixed metal oxide catalysts [29,31], the catalyst efficiency is still not high enough. For instance, Lin [19] reported an AA yield of 42% on a fabricated MMO catalyst, the AA formation rate, however, is remarkably low (4.1 $\mu mol\, g^{-1}\, min^{-1}$). Apparent AA yield is strongly dependent upon the operating parameters such as feed composition, space velocity, etc. [14].

It has been recognized that the preparation chemistry of MMO catalysts is rather complicated. Catalyst nature is very sensitive to preparing parameters and the "window" of synthesizing active catalyst is narrow. Thus the reproducibility of catalyst structure/performance is poor. The active catalysts generally consist of Mo and V elements which are also found in catalysts used for the oxidation of propylene to acrolein and that of acrolein to AA [26–33]. To date, the catalysts comprising Mo–V–Te–Nb are found to be superior to those of other

* Corresponding author at: Department of Chemistry, Nanjing University, 22 Hankou Road, Nanjing 210093, China. Tel.: +86 25 83686270; fax: +86 25 83317761.
E-mail address: jiwj@nju.edu.cn (W.-J. Ji).

1381-1169/$ – see front matter © 2006 Elsevier B.V. All rights reserved.
doi:10.1016/j.molcata.2006.11.047

constitution for one-step propane oxidation. It was believed that Mo/V components are responsible for propane activation, and this has been proved in the oxidative dehydrogenation of ethane and propane [39]. Adding Nb into catalyst stabilized the unique catalyst structure, but the catalyst comprising Mo–V–Nb showed no activity for AA formation [32,39]. Only co-presence of Te and Nb or Te and Sb can promote AA production [19,40–42]. However, significant variations in catalyst performance have been observed over the MMO catalysts with identical Mo–V–Te–Nb compositions [14,15,19,21,23–25,38–44], suggesting that there are intrinsic alterations in catalyst nature upon different preparation approaches. For example, TeO_2 was commonly used for preparing Mo–V–Te catalyst while H_6TeO_6 was generally adopted for synthesizing Mo–V–Te–Nb catalyst via hydrothermal preparation approach [14,16–18,21,44]. It is necessary to demonstrate the chemistry for fabrication in order to gain better understanding of the key issues that control the nature of mixed metal oxide catalysts. In the present study, we systematically investigated the effects of the source of Te and the dispersion of TeO_2 on preparing Mo–V–Te and Mo–V–Te–Nb MMO catalysts for propane oxidation to AA. We envisage that the dispersion of TeO_2 in preparation medium is a critical factor for successful fabrication. We specially adopted the ultrasonic-assisted dispersion of TeO_2 to investigate the issue and obtained meaningful results.

2. Experimental

2.1. Catalyst preparation

There are totally six batches of samples that have been prepared. The information on the preparation conditions and the characteristics of the samples is given in Table 1. The starting material of Te element for catalyst fabrication is TeO_2 purchased from Shanghai Chemical Reagent Company Ltd. (SCRC, 99.9%) or Aldrich Chemical Company Ltd. (ACC, 99.995%). For comparison purpose, H_6TeO_6 was also used in several cases and it was purchased from Aldrich Chemical Company Ltd. (99.999%).

Take the preparation of $Mo_{0.6}V_{0.3}Te_{0.1}O_x$ catalyst as an example:

10.59 g ammonium paramolybdate was dissolved in 104 ml de-ionized water under stirring at room temperature, and 1.60 g TeO_2 was added to the solution leading to the formation of a white suspension, which was kept stirring for 30 min. 6.50 g vanadyl sulfate (the content of H_2O was determined by TG

Table 1
The preparation conditions and the characteristics of the various samples

Catalyst	Composition (nominal)[a]	Te source	Reagent maker	Ultrasonic treatment	Composition (measured)[b]	S.A. (m^2/g)
First batch						
A1[c]	1.00/0.50/0.16	TeO_2	SCRC	No	1.00/0.41/0.04	18.1
A1*[d]	1.00/0.50/0.16	TeO_2	SCRC	No	1.00/0.26/0.09 (1.00/1.34/0.50)[e]	3.5
B1 (pH 2.8)[d]	1.00/0.50/0.16	TeO_2	SCRC	Yes/30 min	1.00/0.26/0.12 (1.00/1.08/0.11)[e]	4.6
C1[d]	1.00/0.57/0.20	TeO_2	SCRC	Yes/30 min	1.00/0.30/0.15 (1.00/2.02/0.52)[e]	2.5
D1[d]	1.00/2.00/0.35	TeO_2	SCRC	Yes/30 min	1.00/0.68/0.35 (1.00/14.3/0.09)[e]	2.1
Second batch						
A2	1.00/0.50/0.16	TeO_2	ACC	No	1.00/0.54/0.16 (1.00/0.48/0.10)[e]	–
B2	1.00/0.57/0.20	TeO_2	ACC	No	1.00/0.66/0.20 (1.00/0.66/0.13)[e]	–
C2 (pH 2.8)[f]	1.00/0.50/0.16	TeO_2	ACC	No	1.00/0.42/0.16 (1.00/0.86/0.02)[e]	–
D2[g]	1.00/0.50/0.16	TeO_2	ACC	No	1.00/0.45/0.15 (1.00/1.14/0.18)[e]	–
Third batch						
A3[g]	1.00/0.57/0.20	TeO_2	ACC	Yes/30 min	1.00/0.22/0.12	2.7
B3	1.00/0.57/0.20	TeO_2	ACC	Yes/30 min	1.00/0.34/0.15	2.4
C3	1.00/0.60/0.17	H_6TeO_6	ACC	Yes/30 min	1.00/0.52/0.17	2.0
Fourth batch						
A4	1.00/0.57/0.20	TeO_2	ACC	Yes/120 min	1.00/0.52/0.19	3.1
Fifth batch						
A5	1.00/0.57/0.20	TeO_2	ACC	Yes/60 min + 60 min	1.00/0.45/0.17	3.8
Sixth batch						
A6	1.00/0.41/0.20/0.16	TeO_2	ACC	Yes/60 min + 60 min	1.00/0.26/0.17/0.16	7.5
A6[h]	1.00/0.41/0.20/0.16	TeO_2	ACC	No		
B6	1.00/0.41/0.20/0.16	H_6TeO_6	ACC	Yes/60 min + 60 min	1.00/0.28/0.17/0.17	3.4
B6[h]	1.00/0.41/0.20/0.16	H_6TeO_6	ACC	No		

[a] The nominal atomic ratio of Mo/V/Te.
[b] The atomic ratio of Mo/V/Te or Mo/V/Te/Nb measured by ICP/XFS.
[c] Activated in flowing Ar.
[d] Activated in static Ar, the same below for the other batches of samples.
[e] The atomic ratio of Mo/V/Te in mother solution.
[f] In case the pH value is indicated, the pH of suspension was adjusted by the 0.5 mol/l $NH_3{\cdot}H_2O$ solution.
[g] Using concentrated solutions for preparation.
[h] Without adopting ultrasonic treatment.

measurement) was dissolved in 60 ml de-ionized water at room temperature to form a deep blue solution that was added dropwisely to the Mo–Te suspension. The mixture changed to viscous brown upon the addition of $VOSO_4$, then to a dark pink suspension. The pH value of the suspension was 2.2. In some cases the pH of suspensions was adjusted to 2.8 with 0.5 mol/l $NH_3{\cdot}H_2O$. The suspension was then poured into Teflon-lined stainless steel autoclaves and maintained at 175 °C for 72 h. The resulting black solids were filtered, washed several times with de-ionized water and dried at 80 °C for 12 h to obtain the catalyst precursor.

In order to modify the dispersion of TeO_2 in the preparation medium, the following procedure was adopted: TeO_2 powder was first wet-milled in an agate mortar for 15–30 min before adding into the solution of $(NH_4)_6Mo_7O_{24}$, and the resulting suspension was subjected to a certain period of ultrasonic-assisted dispersion. And then the solution of $VOSO_4$ was added in under stirring. A certain period of ultrasonic treatment may also be applied after the addition of $VOSO_4$.

The catalyst precursor was activated in the quartz sample container placed in a quartz tubular reactor. Generally, the sample was first purged in flowing Ar (50 ml/min) for 100 min, and then the temperature was ramped to 600 °C at a rate of 5 °C/min and kept at this temperature for 2 h then cooled down in Ar atmosphere. In order to minimize the segregation and loss of TeO_2 component, the precursor was usually calcined in a covered container (static) Ar atmosphere. For comparison proposes, some of the precursors were also calcined in a flowing Ar atmosphere (50 ml/min). In some cases, a pre-calcination of precursors at 280 °C in air was adopted for comparison.

The preparation of Nb-containing catalysts with the nominal constitution of $Mo_{1.00}V_{0.41}Te_{0.20}Nb_{0.16}O_x$ is essentially the same as that of Mo–V–Te MMO with the exception that a certain amount of ammonium niobium oxalate was added at the final stage followed by 60-min ultrasonic treatment. Both TeO_2 and H_6TeO_6 were used as the Te source in preparation.

2.2. Characterization

The specific surface area of the activated catalysts was measured by means of BET method on ASAP2000 apparatus (Micromeritics). The bulk elemental composition of catalysts was examined by inductively coupled plasma (ICP) or X-ray fluorescence analyzer (ARL-9800, ARL, Swiss). Powder X-ray diffraction was conducted using a Rigaku automatic diffractometer (Rigaku D-MAX) with monochromatized Cu Kα radiation (λ = 0.15406 nm) at a setting of 30 kV. XPS measurement was performed using an X-ray photoelectron spectrometer VG ESCALAB Mark II with 1253.6 eV (Mg Kα) radiation at a setting of 10 kV and 15 mA. The binding energy (BE) was calibrated against the C 1s signal (284.6 eV) of contaminant carbon. The surface elemental concentrations were estimated on the basis of the corresponding peak areas being normalized by using the Wagner Factor database. The morphology of the samples was examined on an X-650 Scanning Electron Microscopy (Jarrel-Ash, USA). Hydrogen and propane temperature-programmed reduction/reaction (TPR) were carried out in the temperature range of room temperature (RT) to 800 °C. 0.1–0.2 g sample in a quartz micro-reactor was purged by following nitrogen at 100 °C for 1 h and cooled down to room temperature prior to TPR experiment. The samples were reduced at a rate of 5–10 °C/min in the mixture of H_2/Ar or propane/Ar with a volume ratio of 7/93 or 4.8/95.2, respectively. Surface acidity of the selected samples was measured by the calorimetric measurement of NH_3 adsorption on the self-assembled calorimeter. Prior to the measurement, the samples were first pretreated at 300 °C in the air flow of 30 ml/min for 1 h and then in the nitrogen flow of 30 ml/min for 0.5 h.

2.3. Reaction study

The evaluation of catalyst activity was conducted on a fixed-bed continuous flow quartz micro-reactor under normal pressure at reaction temperatures in the range of 340–420 °C and gas hourly space velocity of 1.5 l/(h g_{cat}). Water vapor was introduced into the reaction system to suppress deep oxidation [35], and the feed composition is $C_3H_8/O_2/H_2O/He = 6/12/40/42$ (v/v/v/v). The outlet is analyzed by on-line GC systems using a 0.32 mm × 25 m HP FFAP capillary column with FID for oxygenates and a Alltech Heyesap D packed column (100/120 mesh, 1/8 in. × 4 m) with TCD for CO_2, propane and propylene. Another 5A molecular sieve packed column (80/100 mesh, 1/8 in. × 2 m) with TCD on the second GC for CO and O_2. A programmed analyzing procedure is applied for FID as well as one TCD: the temperature is kept at 40 °C for 5 min and then ramped to 140 °C at a rate of 5 °C/min and keep for 20 min.

3. Results and discussion

3.1. BET and ICP/XRF measurements

The bulk composition and surface area of the samples prepared by using TeO_2 purchased from SCRC are present in Table 1. The compositions of the mother solutions are also measured and indicated in Table 1. Generally, the surface areas of the samples are in the range of 2–5 m^2/g. From Table 1, one can see that the loss of Te component is obvious on the A1 and A1* samples prepared by using TeO_2 without any modification. Adopting wet milling of TeO_2 and ultrasonic treatment of suspension in preparation significantly decreased the loss of Te (samples B1, C1 and D1). Increasing the V/Mo atomic ratio seems to reduce the loss of Te but enhance the loss of V (sample D1). These deductions are in agreement with the measured composition of the mother solutions.

The chemical compositions of the second batch of MMO samples prepared by using TeO_2 purchased from Aldrich without any modification (wet milling and ultrasonic treatment) are shown in Table 1. One can see that the measured compositions are very close to the feeding ratios, suggesting that the loss of constituents becomes insignificant. The measured Mo/V/Te ratios of the mother solutions also support this deduction. From Table 1, an interesting finding is that the samples subject to static (samples A2–D2) and flowing (not included in Table 1) calcinations showed very similar chemical compositions, indicating that even in a flowing atmosphere there is little Te loss. This is largely

different from the observation made in the first batch of preparation, suggesting the nature of TeO_2 has a remarkable impact on the character of final sample. The nature of TeO_2 can have a direct impact on its dispersion in preparation medium, which in turn affects precipitation/condensation of the constituents during hydrothermal process; as a consequence, the segregation of Te could be different.

From the above investigations one can see that the source of TeO_2 can have an impact on the properties of final samples. The third batch of samples was prepared by using TeO_2 (Aldrich) with wet milling and ultrasonic treatment. The major difference in preparing the third batch of samples is the concentration of solutions: more concentrated solutions were used for preparing the A3 sample [17]. The BET surface areas and chemical compositions of the samples are presented in Table 1. The surface areas of A3 and B3 are ~2.5 m^2/g, slightly smaller than the reported values [16,17]. The loss of Te is insignificant while that of V is noticeable after the hydro-thermal process, suggesting that the applied ultrasonic treatment has an effect on not only the dispersion of TeO_2 in preparation medium, but also the precipitation of other constituent during hydrothermal procedure. In addition, using more concentrated solutions in preparation seemed to cause a more pronounced loss of V (A3). In case H_6TeO_6 (Aldrich) was used as the Te source for fabricating Mo–V–Te MMO, the resulting sample (C3) has a surface area of 2.0 m^2/g; closing to that of A3 and B3. The measured composition of C3 is quite similar to its nominal value for preparation.

The fourth batch of samples was prepared to study the effect of the period of ultrasonic treatment on catalyst property. The surface area of the A4 sample is 3.1 m^2/g; similar to that of the third batch of samples. The content of Te and V in A4 is basically retained after the hydro-thermal treatment (Table 1).

The fifth batch of Mo–V–Te catalyst was prepared by integrating the beneficial aspects released in the preceding investigations. The surface area of the resulting sample (A5) is 3.8 m^2/g; slightly higher than that of the third and fourth batches of samples. The measured composition indicates a small fraction of V and Te is lost after the hydrothermal procedure.

The surface areas of the Mo–V–Te–Nb catalysts are in the range of 3.4–7.5 m^2/g (Table 1). The B6 catalyst prepared by using H_6TeO_6 as the Te source has comparatively lower surface area (3.4 m^2/g versus 7.5 m^2/g). Adding Nb into the catalyst slightly increases the surface area and this has been observed by other researchers [14,17,18,21,44]. Using H_6TeO_6 for catalyst fabrication suppresses the loss of V in the sample (B6 as well as C3). The content of Te and Nb maintains while that of V decreases somehow in the final catalysts.

3.2. XRD and H_2/C_3H_8-TPR

It has been argued that there is a mixture of orthorhombic (M1)/hexagonal (M2) phases in the Mo–V–Te catalysts [24,40,44–49,52], and the existence of the orthorhombic phase is critical [17,20,40]. The XRD results (not shown) indicate that there is little orthorhombic phase but a large amount of MoO_3 as well as hexagonal phase in the first batch of samples [52,54–56]. The phase composition of A1 calcined in flowing

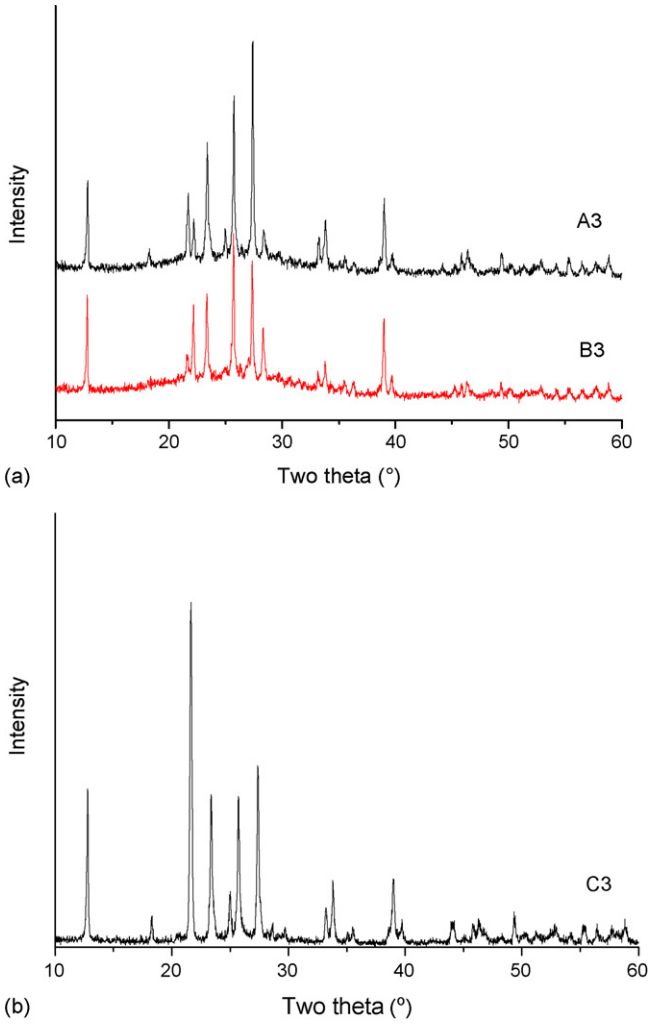

Fig. 1. XRD patterns of the third batch of samples: (a) A3 and B3 and (b) C3.

Ar is entirely different from that of others activated in static atmosphere because there is a significant Te loss in the A1 sample. The second batch of samples activated in static and flowing Ar also show mostly the features of MoO_3/hexagonal phases. The orthorhombic phase is absent in these samples. The XRD results of the A3 and B3 samples are different from that of the second batch of samples (Fig. 1), the orthorhombic phase can be observed in the A3 sample. If H_6TeO_6 was used instead of TeO_2 as the Te source and the ultrasonic treatment was adopted in preparation, the resulting sample (C3) contains a large amount of MoO_3/$(V_{0.07}Mo_{0.93})_5O_{14}$ [JCPDS: 31-1437] phases [17,52,56], indicating that there is an obvious phase segregation in the sample. The XRD pattern of the A4 sample (Fig. 2a) shows that the amount of orthorhombic phase is diminished while that of hexagonal/$TeVO_4$ phases is increased [16,17,40,56]. Poor baseline indicates there might be amorphous species in the sample. The results suggested that an over-ultrasonic treatment would induce a negative effect on the formation of orthorhombic phase. Fig. 2b clearly shows that there is a large amount of M1 + M2 phases in the A5 sample [40], indicating a proper ultrasonic-assisted dispersion of TeO_2 favors the formation of efficient phase mixture. It is found that using both H_6TeO_6 and

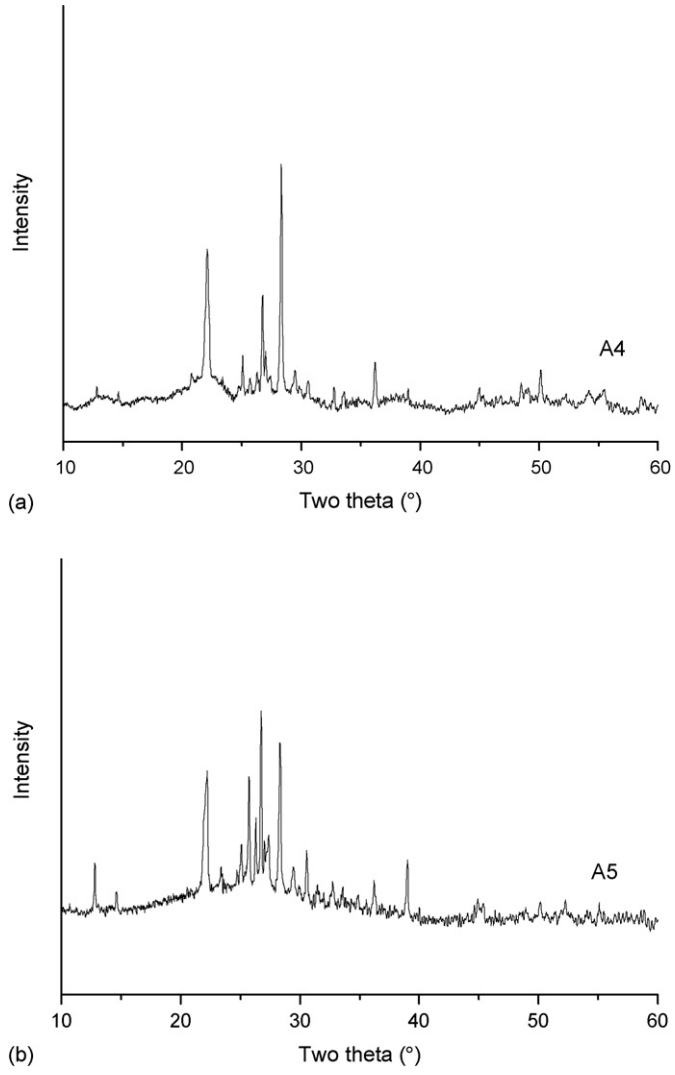

Fig. 2. XRD patterns of (a) the fourth batch and (b) the fifth batch of samples.

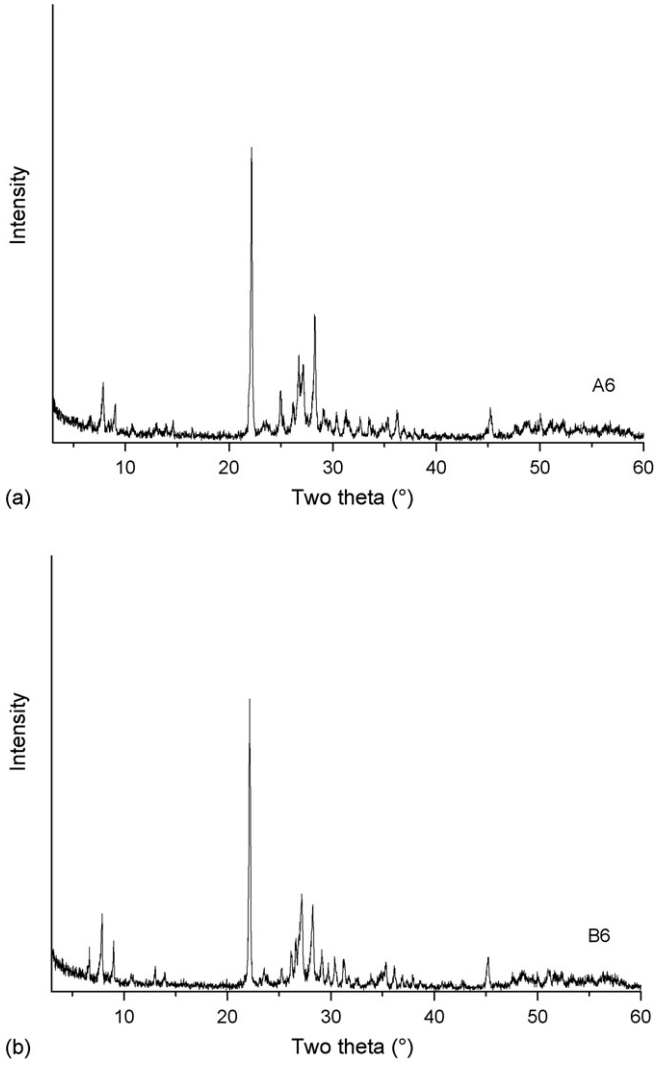

Fig. 3. XRD patterns of the samples of (a) A6 and (b) B6.

TeO_2 as the Te source with ultrasonic treatment in preparing Mo–V–Te–Nb catalysts yields nearly identical phase composition (Fig. 3). There is dominant M1 and certain amount of M2 phases existing in the A6 and B6 samples [17,40,53,54,58]. This is considerably different from the situation observed on the Mo–V–Te system.

H_2-TPR examination reveals that the reduction behavior of A3 (Fig. 4a) is notably different from that of the first and second batches of samples, corresponding to the variation of phase composition. The reduction behavior of the C3 sample prepared with H_6TeO_6 (Fig. 4a) resembles that of the second batch of samples, coincident with the XRD results. The reduction behavior of the A4 and A5 samples is similar (Fig. 4b) with the exception that the shoulder at ca. 533 °C is considerably intensive on the latter catalyst. The shoulder is attributable to the reduction of Te^{4+} species while the main reduction peaks beyond 600 °C can be ascribed to the reduction of M^{6+}/V^{5+} species to Mo^{x+} ($x<6$)/V^{x+} ($x<5$) ones.

For the Nb-containing catalysts not only the reactivity but also the reducibility of lattice oxygen is significantly enhanced (Fig. 4c). The C_3H_8-TPR results obtained on A6 and B6 are shown in Fig. 5. In terms of the amount of C_3H_8 consumption and CO_x generation, the A6 and B6 catalysts are the most active and selective ones among all of the catalysts examined.

3.3. Calorimetric measurement

The MMO catalysts for propane partial oxidation are multifunctional, and surface acidity is one of the critical characters for the reaction [30,32,41,42]. Calorimetric measurement of NH_3 probe was employed to gain the information on surface acidity of the selected catalysts.

NH_3 adsorption over the A3 sample shows the initial adsorption heats of ~100 kJ/mol and fairly high NH_3 coverage (Fig. 6), suggesting that the catalysts are acidic with high density of acid sites. Increment in the number of acid sites with certain acidity may be beneficial for the target reaction [41,42]. Note that when H_6TeO_6 was used as the Te source in preparing three-constituent Mo–V–Te catalyst, the resulting sample (C3) showed no surface acidity (Fig. 6). However, if H_6TeO_6 was adopted in preparing four-constitute Mo–V–Te–Nb catalyst,

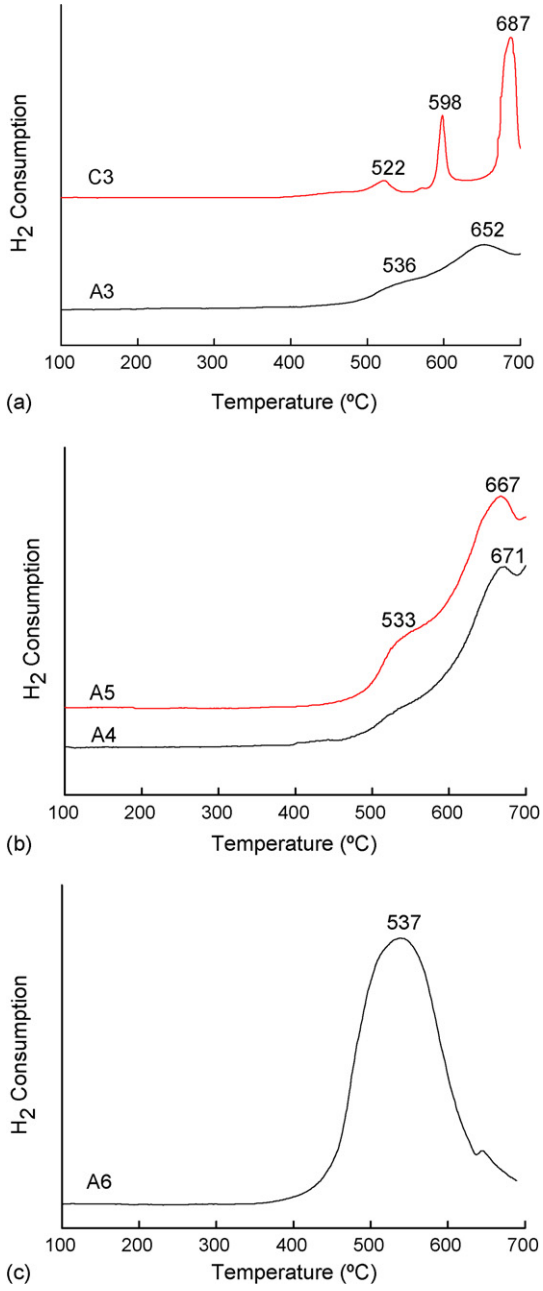

Fig. 4. H_2-TPR profiles of the samples of (a) A3 and C3; (b) A4 and A5 and (c) A6.

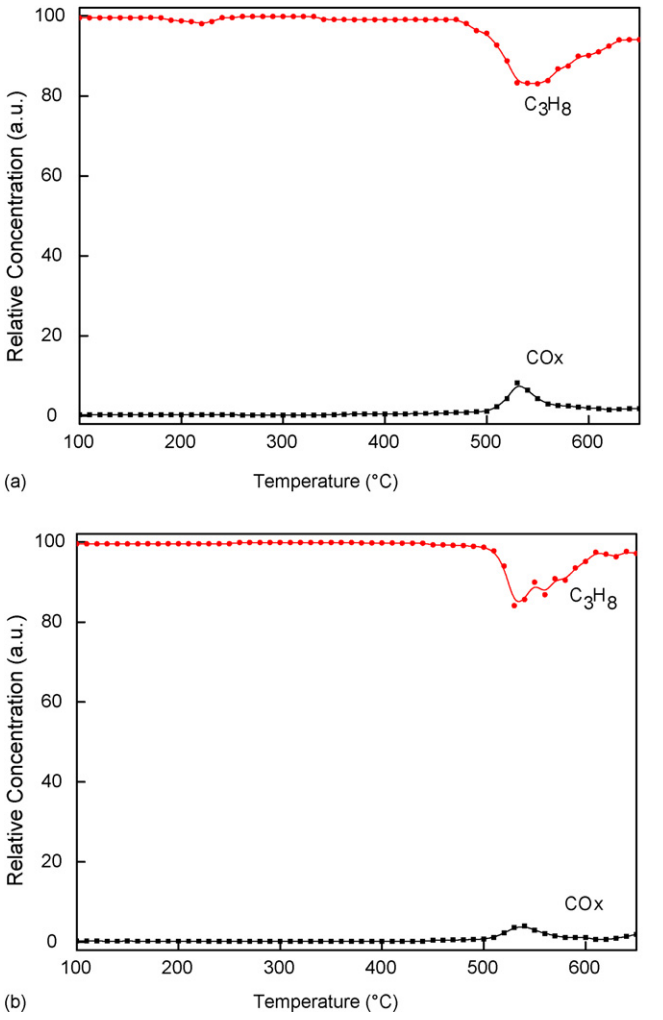

Fig. 5. Propane consumption and carbon oxides formation in C_3H_8-TPR on the samples of (a) A6 and (b) B6.

the obtained sample (B6) showed medium surface acidity (see below).

For the A4 sample, the initial adsorption heat (~80 kJ/mol) is slightly lower than that of A3 and the surface density of acid sites is similar to that of A3 (not shown). The measured surface acidity of the A4 sample seems not to change notably with the phase composition. The initial adsorption heat on the A5 sample is ca. 105 kJ/mol (Fig. 6), and the coverage of acid sites is slightly higher than that of A3. Overall, the surface acidity of A3 and A5 is rather comparable in terms of initial adsorption heat as well as NH_3 coverage (Fig. 6).

Introducing Nb component into the catalysts slightly decreased the initial adsorption heats to ca. 60 kJ/mol; in

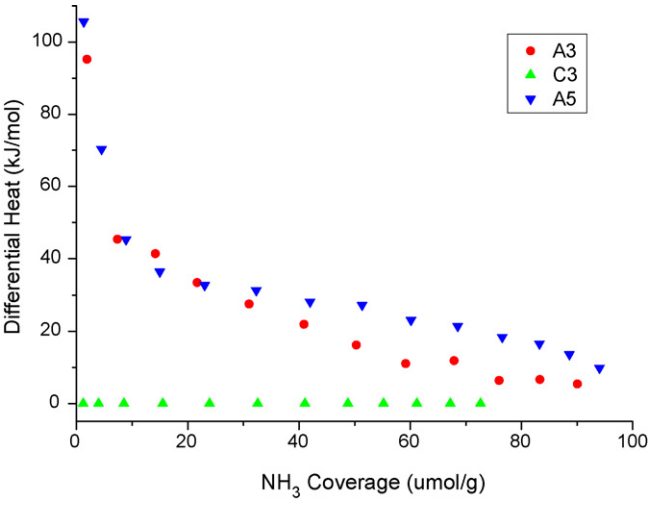

Fig. 6. The differential adsorption heats with NH_3 coverage over the A3, C3 and A5 samples.

Table 2
The surface properties of the Mo–V–Te–Nb catalysts measured by XPS

Sample	Binding energy (eV)				Surface composition
	Mo $3d_{5/2}$	V $2P_{3/2}$	Te $3d_{5/2}$	Nb $3d_{5/2}$	
A6 (precursor)	232.7	516.3	576.3	206.9	$Mo_{1.00}V_{0.18}Te_{0.48}Nb_{0.17}O_x$
A6 (activated)	232.5	516.0	576.1	206.7	$Mo_{1.00}V_{0.22}Te_{0.46}Nb_{0.21}O_x$ ($Mo_{1.00}V_{0.41}Te_{0.20}Nb_{0.16}O_x$)[a]
B6 (precursor)	232.7	516.4	576.3	207.0	$Mo_{1.00}V_{0.15}Te_{0.49}Nb_{0.19}O_x$
B6 (activated)	232.6	516.4	576.3	207.0	$Mo_{1.00}V_{0.15}Te_{0.47}Nb_{0.18}O_x$ ($Mo_{1.00}V_{0.41}Te_{0.28}Nb_{0.17}O_x$)[a]

[a] Those are the bulk compositions measured by XRF.

Table 3
The catalytic activities of A1, B1 and C1 samples at 380 °C

Catalyst	Conversion (%)	Selectivity (mol%)						AA yield (mol%)
		AA[a]	ACT[b]	ACR[c]	AcOH[d]	$C_3^=$[e]	CO_x	
A1	56.6	0.0	0.0	0.0	13.2	5.5	81.3	0.0
B1	10.4	12.3	0.0	0.6	9.9	38.4	38.8	1.3
C1	26.1	11.4	0.0	1.2	11.8	33.4	42.2	3.0

[a] Acrylic acid.
[b] Acetone.
[c] Acrolin.
[d] Acetic acid.
[e] Propylene.

contrast, the surface density of acidic sites (with heats ≥30 kJ/mol) is drastically increased on these Nb-containing catalysts (Fig. 7). Moreover, the surface acidity of the Mo–V–Te–Nb catalysts is little influenced by using different Te source in preparation, coincident well with the XRD observations.

3.4. SEM

The SEM image of the A5 sample is shown in Fig. 8a. The observed morphology is typically analogous to that previously reported [16]. The SEM images of the Nb-containing catalysts (A6 and B6) prepared by means of ultrasonic treatment are shown in Fig. 8b and c. The presence of orthorhombic phase with fractured feature and smaller dimension is clearly observed [17,18,44], and this could be the result of ultrasonic treatment.

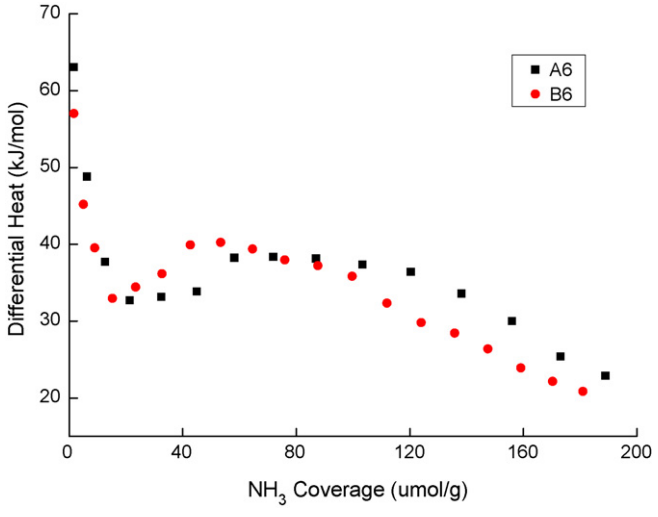

Fig. 7. The differential adsorption heats with NH_3 coverage over the A6 and B6 samples.

3.5. XPS

The results obtained on the Mo–V–Te–Nb catalysts before and after calcination are presented in Table 2. One can see that for both the precursors and activated samples, the surface concentration of V is comparatively lower than that of bulk phase; while that of Te is significantly enriched. Such enrichment of Te element was not observed before on the type of Mo–V–Te–Nb catalysts [21,57], possibly due to the employment of ultrasonic treatment. For the A6 catalyst prepared with TeO_2, the surface concentration of Nb is slightly higher than that in bulk, while for the B6 catalyst prepared with H_6TeO_6, the surface as well as bulk concentration of Nb is essentially the same. In addition, using different source of Te for preparing Mo–V–Te–Nb catalyst shows little impact on the surface Te concentration.

From Table 2, the binding energies (BEs) of the elemental constituents in both precursors and activated catalysts are very similar, suggesting that the oxidation state of the elements is essentially retained after calcinations. In view of the BEs of Mo, V, Te and Nb elements of the MMO catalysts reported in the literature [47] and those in the reference compounds [58], the constituents of Mo, V, Te and Nb in the A6 and B6 catalysts are mostly in the form of Mo^{6+}, V^{5+}, Te^{4+} and Nb^{5+}, respectively. Even though H_6TeO_6 was used as the Te source, the oxidation state of Te in the activated sample is approximately 4+; this is because the Te^{6+} species can be converted to Te^{4+} species at higher temperature calcination (600 °C) in Ar atmosphere.

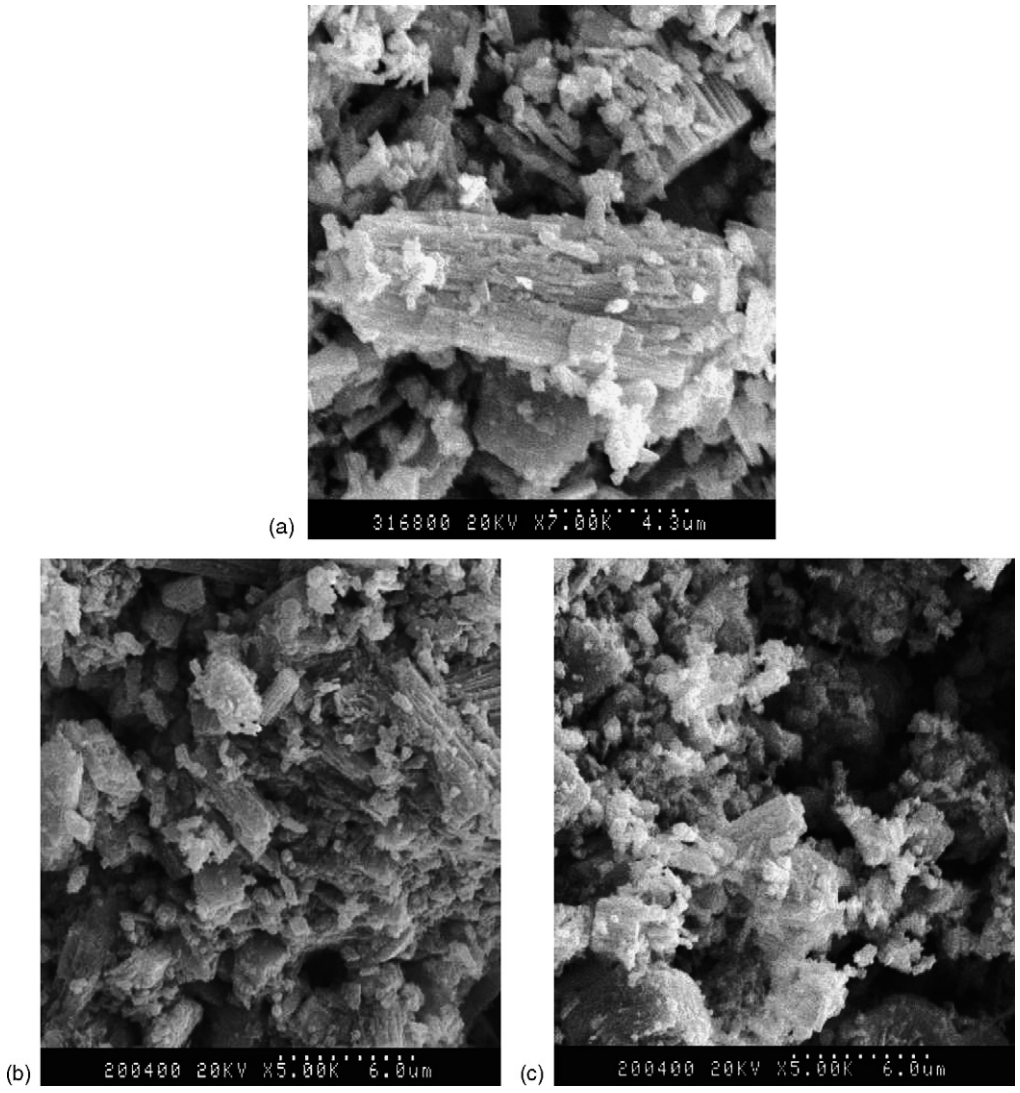

Fig. 8. The SEM images of the samples of (a) A5, (b) A6 and (c) B6.

3.6. Catalyst activity

The catalyst performances of A1, B1 and C1 at the typical reaction temperature of 380 °C are presented in Table 3. The overall performances are poor; and this is due to the lack of essential orthorhombic phase in the samples [52]. The highest AA yield is 3.0 mol% obtained on catalyst C1 at 380 °C. The second batch of samples activated in both static and flowing Ar are found to be inactive for the reaction. The highest propane conversion is less than 3%. The poor performance can be reasonably explained by the absence of essential orthorhombic phase and extremely low surface acidity of the samples.

The typical reaction data of the third and fourth batch of samples are shown in Table 4. A3 shows the highest AA yield of 13 mol% at 390 °C with 57.2% propane conversion; while B3 has the highest AA yield of 2.2 mol% at identical reaction temperature. The results indicate that catalyst efficiency is influenced by not only the dispersion of TeO_2 but also the concentration of starting materials in preparation. The results also indicated that the presence of orthorhombic phase is critical and that the moderate surface acidity may be favorable for AA formation. The catalytic activity of C3 is awfully poor (∼2.7% conversion with no AA selectivity), indicating that using H_6TeO_6 as the Te source is invalid to obtain active Mo–V–Te catalyst via hydrothermal approach. The ineffectiveness of the H_6TeO_6-derived Mo–V–Te catalyst is understandable in terms of the results of XRD (severe phase segregation) and calorimetric measurement (non-acidic). Only 4.3% AA yield was obtained on the A4 catalyst (Table 4), this is because an over-ultrasonic treatment favors the generation of hexagonal phase rather than orthorhombic one.

Shown in Table 5 is the reaction data of the A5 catalyst. An AA yield of 16.2% can be achieved at 400 °C. The better performance of A5 implies that the strategy adopted for catalyst fabrication is workable. The reaction performances of the Nb-containing MMO catalysts are summarized in Table 6. At 45–50% propane conversion, AA selectivity reaches ca. 60%, much better than that of the Mo–V–Te catalyst system. Generally speaking, A6 is less active but slightly selective than B6, and the performances at the typical reaction temperature of 380 °C

Table 4
The catalyst activities of A3, B3 and A4 samples at 390 °C

Catalyst	Conversion (%)	Selectivity (mol%)						AA yield (mol%)
		AA	ACT	ACR	AcOH	$C_3^=$	CO_x	
A3	57.2	22.7	0.0	0.7	12.8	11.0	52.7	13.0
B3	12.5	17.9	0.0	0.6	12.5	33.3	30.4	2.2
A4	17.5	24.6	0.0	0.0	7.8	15.2	52.5	4.3

Table 5
The catalyst activity of the A5 sample

Temperature (°C)	Conversion (%)	Selectivity (mol%)						AA yield (mol%)
		AA	ACT	ACR	AcOH	$C_3^=$	CO_x	
360	31.5	41.6	0.0	0.5	11.6	14.7	31.6	13.1
380	40.4	37.2	0.0	0.3	8.4	10.9	43.2	15.0
390	46.9	33.3	0.0	0.2	6.9	8.1	50.6	15.6
400	55.3	29.3	0.0	0.1	5.6	7.4	57.6	16.2

Table 6
The catalyst activities of the A6 and B6 samples with and without ultrasonic treatment

Temperature (°C)	Conversion (%)	Selectivity (mol%)						AA yield (mol%)
		AA	ACT	ACR	AcOH	$C_3^=$	CO_x	
A6								
360	32.4	63.2	0.0	0.3	5.7	10.3	20.4	20.5 (12.6)[a]
380	50.5	56.7	0.0	0.1	5.0	5.5	32.7	28.6 (17.6)
400	65.4	37.5	0.0	0.1	2.2	3.7	56.5	24.6 (15.2)
B6								
360	45.6	62.4	0.0	0.2	3.1	8.1	26.2	28.4 (17.5)
380	59.3	51.8	0.0	0.1	1.8	5.0	41.3	30.8 (19.0)
400	71.3	21.9	0.3	0.2	4.9	2.6	70.1	15.6 (9.6)
A6[b]								
360	20.2	65.5	0.0	1.6	6.0	17.4	9.5	13.2 (8.1)
380	29.7	65.9	0.0	0.5	5.0	12.4	16.2	19.6 (12.1)
400	41.1	60.7	0.3	0.2	3.1	7.1	28.9	25.0 (15.4)
B6[b]								
360	29.6	58.8	0.0	0.6	10..3	12.0	18.3	17.4 (10.7)
380	42.6	63.9	0.0	0.2	3.9	8.0	24.0	27.2 (16.8)
400	57.0	48.6	0.3	0.1	1.9	5.2	44.2	27.7 (17.1)

[a] The numbers indicated in the parentheses are the AA formation rate (μmol g^{-1} min^{-1}).
[b] Without adopting ultrasonic treatment.

are rather comparable (Table 6). This is notably differing from the situations observed over the Mo–V–Te system. First of all, introducing Nb component into the catalyst can not only suppress the phase segregation but also stabilize the orthorhombic Mo–V–Te–Nb phase. Secondly, in the case of TeO_2 being used as Te source, the ultrasonic treatment can significantly enhance the dispersion of tellurium; on the other hand, since telluric acid is soluble in water, the applied ultrasonic treatment has little effect on its "dispersion"; however, ultrasound is a type of energy which can still accelerate the interaction between the different constituents existing in the preparation medium. Finally, the employment of ultrasonic treatment probably has an effect on the dispersion of niobium which suppresses the growth of the needle-like particles of the active orthorhombic phase (refer to Fig. 8b and c), resulting in the generation of more (1 1 0) faces on the basis of per unit mass of catalyst [40,52]. This may account for the enhanced performances of the Mo–V–Te–Nb catalysts fabricated by adopting ultrasonic treatment (Table 6).

4. Concluding remarks

In this study, different source of Te (different TeO_2 as well as H_6TeO_6) was used to fabricate the Mo–V–Te and Mo–V–Te–Nb MMO catalysts for one-step oxidation of propane to AA. The major concern is the effect of nature of Te source and dispersion of TeO_2 in preparation media on catalyst characteristics and performance. Wet-milling of TeO_2 powder and ultrasonic-treatment of suspension mixture were specially adopted to modify the dispersion of TeO_2. It has been demonstrated that the dispersion of TeO_2 in preparation media is a critical factor for

successful catalyst fabrication, and the extent of TeO_2 dispersion can be effectively enhanced by applying a certain period of ultrasonic treatment on TeO_2-containing suspension. Using different source of Te in preparation can affect on the interaction between the constituents and on the precipitation/condensation of components during hydrothermal process, causing significant alterations in (i) phase composition/segregation, (ii) bulk/surface elemental concentration, (iii) reactivity of lattice oxygen, and (iv) surface acidity of the MMO catalysts, and consequently in their catalyst performances. With a proper ultrasonic treatment, an active and selective Mo–V–Te–Nb catalyst can be obtained even if TeO_2 is used as the Te source for catalyst preparation. When H_6TeO_6 was used as the Te source, an enhancement of catalyst performance can also be observed by adopting ultrasonic treatment.

Acknowledgments

Financial supports from Rohm & Haas, BASF and the Ministry of Science and Technology of China (Grant 2000048009) are gratefully acknowledged. We also appreciate the support of Modern Analytic Center of Nanjing University for catalyst characterizations and kind help from Prof. J.Y. Shen and L. Dong.

References

[1] H.H. Kung, Adv. Catal. 40 (1994) 1.
[2] S. Albonetti, F. Cavani, F. Trifiro, Catal. Rev.-Sci. Eng. 38 (1996) 413.
[3] A.T. Bell, Science 299 (2003) 1688.
[4] Catal. Lett. 67 (1.) (2000) (special issue).
[5] X.G. Yang, T.Z. Liu, Chem. Tech. Nat. Gas 23 (1998) 43 (in Chinese).
[6] M. Ai, J. Catal. 101 (1986) 389.
[7] H. Cheng, Y.F. Han, H.M. Wang, Petrochem. Tech. 28 (1999) 803 (in Chinese).
[8] Y.F. Han, H.M. Wang, H. Cheng, J.F. Deng, Chem. Commun. 521 (1999).
[9] B. Kerler, A. Martin, M.M. Pohl, M. Baerns, Catal. Lett. 78 (2002) 259.
[10] H.S. Jiang, X. Mao, S.J. Xie, B.K. Zhong, J. Mol. Catal. A 185 (2002) 143.
[11] N. Mizuno, M. Tateishi, M. Iwamoto, Appl. Catal. A 128 (1995) 165.
[12] N. Dimitratos, J.C. Vedrine, J. Mol. Catal. A: Chem. 255 (2006) 184.
[13] N. Dimitratos, J.C. Vedrine, Appl. Catal. A: Gen. 256 (2003) 251.
[14] E. Balcells, F. Borgmeier, I. Gribtede, H.-G. Lintz, F. Rosowski, Appl. Catal. A 266 (2004) 211.
[15] B.C. Zhu, H.B. Li, W.S. Yang, L.W. Lin, Catal. Today 93 (2004) 229.
[16] J.N. Al-Saeedi, V.V. Guliants, O. Guerrero-Perez, M.A. Banares, J. Catal. 215 (2003) 108.
[17] D. Vitry, Y. Morikawa, J.L. Dubois, W. Ueda, Appl. Catal. A 251 (2003) 411.
[18] J.M. Lopez-Nieto, P. Botella, B. Solsona, J.M. Oliver, Catal. Today 81 (2003) 87.
[19] M.M. Lin, Appl. Catal. A 250 (2003) 305.
[20] J.M.M. Millet, H. Roussel, A. Pigamo, J.L. Dubois, J.C. Jumas, Appl. Catal. A 232 (2001) 77.
[21] P. Botella, J.M. Lopez-Nieto, B. Solsona, A. Mifsud, F. Marquez, J. Catal. 209 (2002) 445.
[22] N. Fujikawa, K. Wakui, K. Tomita, N. Ooue, W. Ueda, Catal. Today 71 (2001) 83.
[23] M.M. Lin, Appl. Catal. A 207 (2002) 1.
[24] K. Asakura, K. Nakatani, T. Kubota, J. Catal. 194 (2000) 309.
[25] H. Watanabe, Y. Koyasu, Appl. Catal. A 194 (2000) 479.
[26] W. Li, K. Oshihara, W. Ueda, Appl. Catal. A 182 (1999) 357.
[27] F. Cavani, F. Trifro, Catal. Today 51 (1999) 561.
[28] R.K. Grasselli, Catal. Today 49 (1999) 141.
[29] M. Lin, M. Linsen, EP Patent 962,253, A2 (1999).
[30] J.C. Vedrine, E.K. Novakova, E.G. Derouane, Catal. Today 81 (2003) 247.
[31] T. Ushikubo, H. Nakamura, Y. Koyasu, S. Wajiki, US Patent 5,380,933 (1995).
[32] J.C. Vedrine, Top. Catal. 21 (2002) 97.
[33] E.K. Novakova, J.C. Vedrine, E.G. Derouane, J. Catal. 211 (2002) 226.
[34] E.K. Novakova, J.C. Vedrine, E.G. Derouane, J. Catal. 211 (2002) 235.
[35] E.K. Novakova, E.G. Derouane, J.C. Vedrine, Catal. Lett. 83 (2002) 177.
[36] P. Botella, P. Concepción, J.M. López Nieto, Y. Moreno, Catal. Today 99 (2005) 51.
[37] R.K. Grasselli, Catal. Today 99 (2005) 23.
[38] J.C.J. Bart, A. Bossi, G. Petrini, G. Battison, A. Castellan, R. Covini, Appl. Catal. 4 (1982) 153.
[39] E. Thorsteinson, T. Wilson, F. Young, P. Kasai, J. Catal. 52 (1978) 116.
[40] M. Baca, A. Pigamo, J.L. Dubois, J.M.M. Millet, Top. Catal. 23 (2003) 39.
[41] R.K. Grasselli, Top. Catal. 15 (2001) 93.
[42] R.K. Grasselli, J.D. Burrington, D.J. Buttrey, P. Desanto Jr., C.G. Lugmair Jr., A.F. Volpe Jr., T. Weingand, Top. Catal. 23 (2003) 5.
[43] K. Oshikara, T. Hisano, W. Ueda, Top. Catal. 15 (2001) 153.
[44] P. Botella, B. Solsona, A. Martinez-Arias, J.M. Lopez-Nieto, Catal. Lett. 74 (2001) 149.
[45] T. Ushikubo, K. Oshima, A. Kayou, M. Hatano, Stud. Surf. Sci. Catal. 112 (1997) 473.
[46] M. Aouine, J.L. Dubois, J.M.M. Millet, Chem. Commun. 1180 (2001).
[47] J.M.M. Millet, H. Roussel, A. Pigamo, J.L. Dubois, J.C. Jumas, Appl. Catal. A 232 (2002) 77.
[48] S. Komada, H. Hinago, M. Kaneta, EP Patent 896,809, A1 (1999).
[49] M. Lin, T.B. Desai, F.W. Kaiser, P.D. Klugherz, Catal. Today 61 (2000) 223.
[50] H. Tsuji, Y. Koyasu, J. Am. Chem. Soc. 124 (2002) 5608.
[51] M.E. Davis, C.J. Dillon, J.H. Holles, J. Labinger, Angew. Chem. Int. Ed. 41 (2002) 858.
[52] E.K. Novakova, J.C. Vedrine, in: J.L.G. Fierro (Ed.), Metal Oxides: Chemistry and Applications, CRC Press, Boca Raton, 2006, pp. 413–461.
[53] P. Botella, E. Garcia-Gonzalez, J.M. Lopez, J.M. Gonzalez-Calbet, Solid State Sci. 7 (2005) 507.
[54] A.F. Wells, Structural Inorganic Chemistry, Oxford University Press, Oxford, 1984.
[55] L. Kihlborg, Acta Chem. Scand. 13 (1959) 954;
L. Kihlborg, Acta Chem. Scand. 23 (1969) 1834.
[56] J.N. Al-Saeedi, Ph.D. Thesis, University of Cincinnati, 2003.
[57] V.V. Guliants, R. Bhandari, H.H. Brongersma, A. Knoester, A.M. Gaffney, S. Han, J. Phys. Chem. B 109 (2005) 10234.
[58] J.F. Moulder, W.F. Stickle, P.E. Sobol, K.D. Bomben, Handbook of X-Ray Photoelectron Spectroscopy, Physical Electronics, 1995.